PHYSICAL REVIEW D **88,** 094014 (2013)

Nonleptonic $B_c \to VV$ decays

Susmita Kar,[1] P. C. Dash,[2,*] M. Priyadarsini,[2] Sk. Naimuddin,[3] and N. Barik[4]

[1]*Physics Department, North Orissa University, Baripada 757003, India*
[2]*Physics Department, Institute of Technical Education and Research, SOA University, Bhubaneswar 751030, India*
[3]*Physics Department, Maharishi College of Natural Law, Bhubaneswar 751007, India*
[4]*Physics Department, Utkal University, Bhubaneswar 751004, India*

(Received 10 July 2013; published 18 November 2013)

We study the exclusive nonleptonic $B_c \to VV$ decays, within the factorization approximation, in the framework of the relativistic independent quark model, based on a confining potential in the scalar-vector harmonic form. The weak form factors are extracted from the overlap integral of meson wave functions derived in the relativistic independent quark model. The predicted branching ratios for different B_c-meson decays are obtained in a wide range, from a tiny value of $\mathcal{O}(10^{-6})$ for $B_c \to D^* D^*_{(s)}$ to a large value of 24.32% for $B_c \to B_s^* \rho^-$, in general agreement with other dynamical-quark-model predictions. The decay modes $B_c \to B_s^* \rho^-$ and $B_c \to B^* \rho^-$ with high branching ratios of 24.32% and 1.73%, respectively, obtained in this model should be detectable at the LHC and Tevatron in the near future. The $b \to c$, u induced decays are predicted predominantly in the longitudinal mode, whereas the $\bar{c} \to \bar{s}$, $\bar{d}$ induced decays are obtained in a slightly higher transverse mode. The CP-odd fractions ($R_\perp$) for different decay modes are predicted and those for color-favored $B_c \to D^* D^*$, $D^* D_s^*$ decays indicate significant CP violation in this sector.

DOI: 10.1103/PhysRevD.88.094014 PACS numbers: 13.25.Hw, 12.39.Pn

I. INTRODUCTION

The discovery of the B_c meson by the CDF Collaboration in 1998 [1] has aroused a great deal of interest in its production mechanism, spectroscopy, and decay properties. Subsequent measurements of its life time τ_{B_c} and mass M_{B_c}—leading to the recent measurements by the CDF and D0 Collaborations of $\tau_{B_c} = 0.45^{+0.073}_{-0.065}\,(\text{Stat}) \pm 0.0036\,(\text{Syst})$ ps [2], $M_{B_c} = (6.2756 \pm 0.0029\,(\text{Stat}) \pm 0.0026\,(\text{Syst})$ GeV [2], and $M_{B_c} = (6.3 \pm 0.014\,(\text{Stat}) \pm 0.005\,(\text{Syst})$ GeV [3]—have opened new windows for the analysis of heavy quark dynamics. At the current level of accuracy, the LHC is expected to produce around 5×10^{10} B_c events per year [4], which would provide important clues to test the standard model predictions on flavor parameters and study the decay properties of the B_c meson.

The B_c-meson decays are of special theoretical interest due to the following characteristic features. 1) Being the lowest bound state of two different heavy quarks with open flavors (b and $\bar{c}$), it cannot annihilate into gluons and is stable against strong and electromagnetic interactions. Hence the B_c meson decays via the weak interaction. 2) Since both of the constituents (b, $\bar{c}$) are heavy, they can each decay individually, yielding rich B_c-meson decay channels. The tree-level B_c-meson decays can be broadly divided into three categories. (i) $b \to q(q = c, u)$ induced decays with the antiquark $\bar{c}$ as the spectator, (ii) $\bar{c} \to \bar{s}$, $\bar{d}$ induced decays with the quark b as the spectator, and (iii) the relatively suppressed weak-annihilation modes. The estimates [4] show that the contribution of the weak annihilation to the total B_c-decay rate is hardly 10%. On the other hand, the contribution of $\bar{c} \to \bar{s}$, $\bar{d}$ and $b \to c$, u induced decay modes are found to be about 70% and 20%, respectively, and hence are competitive in magnitude.

In $\bar{c} \to \bar{s}$, $\bar{d}$ induced decay modes, the four-momentum transfer squared q^2 varies from $q^2 \to 0$ to $q^2_{\max} = 1$ GeV^2 only, whereas the allowed kinematic range for $b \to c$, u induced modes vary from $q^2 \to 0$ to $q^2_{\max} = 10$ GeV^2 and $q^2 \to 0$ to $q^2_{\max} = 18$ GeV^2, respectively, for a B_c meson decaying to charmonium and D-meson states. It is worthwhile to consider both categories of constituent-level decays in order to analyze the exclusive two-body nonleptonic B_c-meson decays.

The analysis of nonleptonic decay is nontrivial as it involves matrix elements of local four-quark operators in the nonperturbative QCD approach, the mechanism of which is not yet clear in the standard model framework. However, if one ignores the weak-annihilation contribution, the description of nonleptonic decays gets simplified by using the so-called QCD factorization approximation [5–9], which works reasonably well in the analysis of heavy-quark physics. In this approach, the matrix element of the local four-quark operator is factorized into single-current matrix elements, which are parametrized in terms of weak form factors and meson-decay constants. This makes the factorization approach an appealing method for studying the nonleptonic decays of heavy-flavored mesons. The nonleptonic decays of heavy-flavored mesons were widely studied [10–43] following the pioneering paper written by Bjorken [44] in 1986, which yielded predictions in a wide range. This may be due to the fact

*purendradash@gmail.com

that the data in this sector are still sparse and the weak form factors have not yet been subjected to stringent scrutiny. The justifications for adopting the factorization approximation were shown in the initial theoretical developments based on the QCD approach in the $\frac{1}{N_c} \to 0$ limit [10], Bjorken's intuitive argument based on color transparency [11], the heavy-quark effective theory (HQET) [12], etc., in the study of energetic nonleptonic B decays only, where strong-interaction effects—such as the final-state interactions, the rescattering of final-state hadrons, and the renormalization-point dependence of amplitudes—were shown to be marginal [13]. Similar arguments, however, may not hold up well here as both of the final-state mesons in $B_c \to VV$ decays are heavy and are expected to be in the region close to zero recoil. Contributions to the decay rate in such decays come from both the longitudinal and transverse polarization parts, which can be measured experimentally. From naive counting rules, the longitudinal polarization fraction in B-meson nonleptonic decays is found to be dominant over the transverse polarization fraction, which needs to be checked in the B_c sector as well. The two-charmed-meson decays of the B_c meson ($B \to D^* D^*_{(s)}$) are of special interest as they provide valuable information on CP violation and possible new physics beyond the standard model.

In our recent study [45] we successfully described two-body nonleptonic B_c-meson decays to pseudoscalar-pseudoscalar (PP), pseudoscalar-vector (PV), and vector-pseudoscalar (VP) modes in the relativistic independent quark model (RIQM) [45–48] based on the confining potential in scalar-vector harmonic form. In its earlier applications the model successfully described a wide range of hadronic phenomena—such as the static properties of hadrons [46]—and various decays [45,47,48], including radiative, weak radiative, rare radiative, leptonic, weak leptonic, semileptonic, nonleptonic, and radiative leptonic decays of hadrons in the light- and heavy-flavor sector. In this paper we would like to extend the applicability of the RIQM to predict—within the factorization approach—the weak form factors, their q^2 dependence in the allowed kinematical range, and the branching ratios of $B_c \to VV$ decays.

In the present analysis we will only consider the contribution of the current-current operator in predicting the tree-level nonleptonic B_c-meson decays (as was done in Refs. [5,18,21,22,26,30,40,49–51]). In evaluating the decay width the contribution of the tree diagram is expected to be dominant. The penguin contribution may be important in evaluating CP violation and when searching for new physics beyond the standard model, which we do not consider in this work. Since the Wilson coefficient of the penguin operator is very small, the corresponding contributions to weak-decay amplitudes only become relevant in rare decays, where the tree-level contribution is either strongly Cabibbo-Kobayashi-Maskawa (CKM) suppressed, as in $\bar{B} \to \bar{K}^* \pi$, or where matrix elements of current-current operators do not contribute at all, as in $\bar{B} \to \bar{K}^* \gamma$ and $\bar{B}^0 \to \bar{K}^0 \phi$ [52]. In this paper we do not consider these decays. The contribution of QCD and electroweak penguin operators has also been shown [15,51] to be too small compared to that of current-current operators due to the serious suppression of CKM elements.

The paper is organized as follows. In the following section we provide general remarks on the factorization hypothesis and nonleptonic decay amplitudes. In Sec. III we briefly describe the RIQM framework and extract the model expressions for the weak-decay form factors and polarized transition amplitudes. The numerical results are described in Sec. IV. Section V embodies our summary and conclusion.

II. FACTORIZATION AND NONLEPTONIC TRANSITION AMPLITUDE

In the factorization approach, the transition amplitude for two-body nonleptonic $M \to V_1 V_2$ decays can be approximated by the product of one-particle matrix elements [5,21,22,45,48] as

$$\begin{aligned}\langle V_1 V_2 | \mathcal{H}_{\rm eff} | M \rangle = \frac{G_F}{\sqrt{2}} V_{q_{1(2)} q'_{1(2)}} V_{q_3 q'_3} [a_1(\mu) \langle V_2 | J^\mu | 0 \rangle \\ \times \langle V_1 | J_\mu | M \rangle + a_2(\mu) \\ \times \langle V_1 | J^\mu | 0 \rangle \langle V_2 | J_\mu | M \rangle],\end{aligned} \tag{1}$$

where $G_{\rm F}$ is the Fermi constant, the V_{ij}'s are CKM matrix elements, and $a_1(\mu)$ and $a_2(\mu)$ are the QCD factors, which are expressed in terms of the Wilson coefficients as

$$\begin{aligned} a_1(\mu) &= C_1(\mu) + \frac{1}{N_c} C_2(\mu), \\ a_2(\mu) &= C_2(\mu) + \frac{1}{N_c} C_1(\mu). \end{aligned} \tag{2}$$

Here N_c denotes the number of colors and $J_\mu \equiv V_\mu - A_\mu \equiv \bar{q}'_{1(2)} \gamma_\mu (1 - \gamma_5) q_{1(2)}$ is the vector-axial current.

In the general case, the renormalization-point (μ) dependence of the product of current-operator matrix elements does not cancel the μ dependence of $a_{1,2}(\mu)$. The nonfactorizable contribution to Eq. (1) must be present in order to make the physical amplitude renormalization-scale independent. In the present analysis, as in Refs. [45,53], the nonfactorizable vertex, penguin, hard spectator corrections, etc., are thought to be incorporated into the effective Wilson coefficients a_i(i = 1, 2). In the present analysis we neglect the so-called W-exchange and annihilation diagrams, since in the limit $M_W \to \infty$, they are connected by a Fierz transformation and are doubly suppressed by a kinematic factor of the order (m_i^2/M^2). We also discard the color-octet currents which emerge after the Fierz transformation of color-singlet operators. Clearly,

these currents violate factorization since they can not provide transitions to the vacuum states.

The hadronic matrix element of the weak current J_μ between the initial and final meson states have the covariant decomposition

$$\langle V_1(\vec{k}) \mid A_\mu \mid M(\vec{p})\rangle = f(q^2)\epsilon^*_\mu + a_+(q^2)(\epsilon^*.p)(p+k)_\mu + a_-(q^2)(\epsilon^*.p)(p-k)_\mu, \quad (3)$$

$$\langle V_1(\vec{k}) \mid V_\mu \mid M(\vec{p})\rangle = ig(q^2) \in_{\mu\nu\rho\sigma} \epsilon^{*\nu}(p+k)^\rho(p-k)^\sigma, \quad (4)$$

where ϵ^* is the polarization vector of the vector meson (V_1). p and k represent the four-momentum of the parent meson (M) and that of the daughter meson (V_1), respectively. With the four-momentum transfer $q = p - k \equiv (E, 0, 0, |\vec{q}|)$ and mass m_{V_1}, the polarization vector associated with "V_1" is taken in the form

$$\epsilon^\pm_\mu \equiv \frac{1}{\sqrt{2}}(0, \mp 1, -i, 0), \qquad \epsilon^L_\mu \equiv \frac{1}{m_{V_1}}(|\vec{q}|, 0, 0, E). \quad (5)$$

The matrix element of the current J^μ between the vacuum and the other vector-meson (V_2) final state can be parametrized in terms of the meson decay constant f_{V_2} as

$$\langle V_2|J^\mu|0\rangle = \epsilon^{*\mu}_{V_2} f_{V_2} m_{V_2}. \quad (6)$$

In the factorization approach, the nonleptonic transition amplitude can be calculated from one of the three possible tree-level Feynman diagrams shown in Fig. 1. The color-favored transitions, corresponding to the diagram depicted in Fig. 1(a), represent "class I" transitions which are characterized by the external emission of a W boson. In these transitions, the factorized amplitude coupled to the QCD factor "a_1" only gives the nonvanishing contribution. On the other hand, the color-suppressed transitions corresponding to the diagram depicted in Fig. 1(b) represent "class II" transitions which are characterized by internal W emission. In such transitions, the nonvanishing contributions to the decay rate come from the factorized amplitude associated with the QCD factor "a_2." Figure 1(c), however, represents "class III" transitions which are due to both color-favored and the color-suppressed diagrams involving external and internal W emission. In such decays the factorized amplitudes corresponding to both of the QCD factors "a_1" and "a_2" contribute coherently to give the transition amplitude. For the color-favored general type of tree-level transition $M \to V_1V_2$ pertaining to "class I" transitions, the decay rate can be written as [48,53]

$$\Gamma = \frac{G_F^2}{16\pi} a_1^2(\mu)|V_{q_{1(2)}q'_{1(2)}} V_{q_3q'_3}|^2 \frac{|\vec{k}|}{M^2}|\mathcal{A}|^2. \quad (7)$$

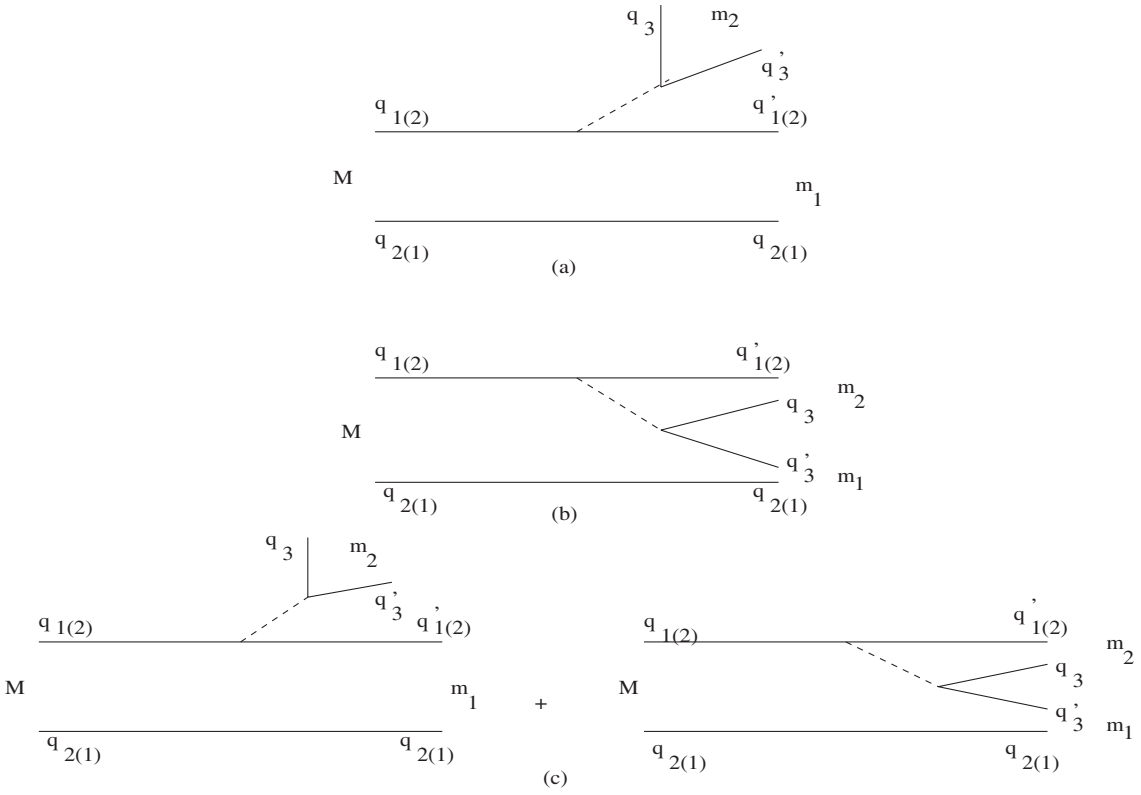

FIG. 1. Quark-level diagram of the nonleptonic decay of a meson $M \to m_1m_2$.

Here M and $\vec{k}$ are taken as the parent-meson mass and three-momentum, respectively, of the recoiled daughter meson "V_1" in the parent-meson rest frame. $|\mathcal{A}|^2$ is the sum of the polarized amplitude squared with $\mathcal{A}_j \equiv \langle V_2|J^\mu|0\rangle\langle V_1|J_\mu|M\rangle$, such that

$$|\mathcal{A}|^2 = \sum_j |\mathcal{A}_j|^2. \tag{8}$$

We use the notation $j = +-, -+$, or ll, where the first and second labels denote the helicity of the V_1 and V_2 meson, respectively.

From the polarized amplitudes expressed in terms of the weak form factors "f," "g," and "a_+" and the decay constant "f_{V_2}" shown in Eqs. (3)–(6), it is straightforward to find the expression for the positive, negative, and longitudinal polarizations, respectively, of the daughter meson V_1 as

$$\begin{aligned}
\mathcal{A}_{+-} &= -f_{V_2} m_{V_2}\{f(q^2) + 2g(q^2)|\vec{k}|M\},\\
\mathcal{A}_{-+} &= -f_{V_2} m_{V_2}\{f(q^2) - 2g(q^2)|\vec{k}|M\},\\
\mathcal{A}_{ll} &= \frac{f_{V_2}}{m_{V_1}}\Big[f(q^2)\Big\{|\vec{k}|^2 + \frac{1}{4M^2}(M^2 + m_{V_1}^2 - m_{V_2}^2)\\
&\quad \times (M^2 + m_{V_2}^2 - m_{V_1}^2)\Big\} + 2a_+(q^2)|\vec{k}|^2 M^2\Big],
\end{aligned} \tag{9}$$

where

$$|\vec{k}| = \left[\left(\frac{M^2 + m_{V_1}^2 - m_{V_2}^2}{2M}\right)^2 - m_{V_1}^2\right]^{1/2}. \tag{10}$$

The decay widths and branching ratios for $B_c \to VV$ decays can be predicted from Eq. (7) using the expressions (8)–(10) for the polarized amplitudes in terms of the weak form factors derivable in the framework of the RIQM.

III. TRANSITION AMPLITUDE AND WEAK-DECAY FORM FACTORS

The color-favored two-body nonleptonic $M \to V_1 V_2$ decays shown in Fig. 1(a) can be described at the constituent level as the decay of one of the constituents (quark/antiquark) $q_{1(2)}$ with four-momentum $p_{q_{1(2)}}$ inside the decaying meson state $|M(\vec{p}, S_M)\rangle$ to a daughter quark/antiquark $q'_{1(2)}$ with momentum $p_{q'_{1(2)}}$, which along with the spectator $q_{2(1)}$ with momentum $p_{q_{2(1)}}$ hadronize to the meson state $|V_1(\vec{k}, S_{V_1})\rangle$. In the process the externally emitted W boson with four-momentum "q" decays to a quark-antiquark pair $(q_3 q'_3)$ which hadronize ultimately to the meson bound state $|V_2(\vec{q}, S_{V_2})\rangle$. Physically, the decay of the hadron takes place in its momentum eigenstate. Therefore, in the present model, the participating meson in a definite momentum $(\vec{p})$ and spin (S_M) state is represented by an appropriate wave packet reflecting the momentum and spin distribution between the quark constituents inside the meson core [45,47,48] as

$$\begin{aligned}
|M(\vec{p}, S_M)\rangle &= \frac{1}{\sqrt{N_M(\vec{p})}} \sum_{\lambda_1,\lambda_2 \in S_M} \zeta^M_{q_1,\bar{q}_2}(\lambda_1, \lambda_2)\\
&\quad \times \int d^3\vec{p}_{q_1} d^3\vec{p}_{q_2} \delta^{(3)}(\vec{p}_{q_1} + \vec{p}_{q_2} - \vec{p})\\
&\quad \times \mathcal{G}_M(\vec{p}_{q_1}, \vec{p}_{q_2}) \hat{b}^\dagger_{q_1}(\vec{p}_{q_1}, \lambda_1) \hat{\bar{b}}^\dagger_{q_2}(\vec{p}_{q_2}, \lambda_2) \mid 0\rangle,
\end{aligned} \tag{11}$$

where $\hat{b}^\dagger_{q_1}(\vec{p}_{q_1}, \lambda_1)$ and $\hat{\bar{b}}^\dagger_{q_2}(\vec{p}_{q_2}, \lambda_2)$ are, respectively, the quark and antiquark creation operators, $\zeta^M_{q_1,\bar{q}_2}(\lambda_1, \lambda_2)$ are the SU(6) spin-flavor coefficients, $N_M(\vec{p})$ is the meson normalization factor, and $\mathcal{G}_M(\vec{p}_{q_1}, \vec{p} - \vec{p}_{q_1})$ is the effective momentum-distribution function defined in terms of momentum probability amplitudes of the quark and antiquark, which is derivable in this model via a momentum-space projection of the bound quark/antiquark eigenmodes. The quark/antiquark energy eigenmodes are obtained by solving the Dirac equation that follows from the independent quark Lagrangian density at the zeroth order with an interaction potential in an equally mixed scalar-vector harmonic form [45,47,48].

In such an approach the invariant transition amplitude is extracted from the S-matrix element by casting it into its standard form only after realizing the energy-momentum conservation through a delta function at the mesonic level. But such a realization at the composite level, starting from a bound constituent-level picture, has never been so straightforward. This is due to the fact that although three-momentum conservation is automatically guaranteed at the mesonic level through the wave packet description (11), it is not so for energy conservation. However, we have shown in Refs. [45,47,48] that energy conservation is also ensured in an average sense by the $\mathcal{G}_M(\vec{p}_{q_1}, \vec{p} - \vec{p}_{q_1})$ used in the wave-packet description (11), where we realized that the expectation value of the sum of the binding energies of the constituent quark and antiquark in the meson bound state in its rest frame is very close to the corresponding observed mass given by

$$\langle M(0)|[E_{q_1}(|\vec{p}_{q_1}|^2 + E_{q_2}(|-\vec{p}_{q_1}|^2)]|M(0)\rangle = M.$$

In this context we assign a running mass $m_{q_1}(\vec{p}_{q_1})$ to the active quark q_1 in the meson state $|M(0)\rangle$, with $m^2_{q_1}(|\vec{p}_{q_1}|) = M^2 - m^2_{q_2} - 2M\sqrt{|\vec{p}_{q_1}|^2 + m^2_{q_2}}$ as an outcome of the energy conservation constraint, $E_{q_1}(|\vec{p}_{q_1}|^2 + E_{q_2}(|-\vec{p}_{q_1}|^2) = M$, while retaining a definite mass m_{q_2} for the spectator q_2. This leads to an upper bound for the quark momentum $|\vec{p}_{q_1}|$ in order to keep $m^2_{q_1}(|\vec{p}_{q_1}|)$ positive definite. In doing so we avoid possible spurious kinematics singularities in the quark-momentum-level integration encountered in our calculation [45,47,48].

Hence our approach in realizing energy-momentum conservation—though it may seem crude and approximate—is no doubt a reasonable approximation. In the absence of any other rigorous field-theoretic method involving bound

constituents, the constituent-level description of decay phenomena of composite hadrons based on such an approximation has provided quite reasonable predictions in our earlier works [45,47,48].

Using the wave-packet description (11) for the parent and daughter meson states, $|M(\vec{p}, S_M)\rangle$ and $|V_1(\vec{k}, S_V)\rangle$, we calculate the S-matrix element using the Feynman technique, and the invariant transition amplitude in the parent-meson rest frame is

$$\mathcal{M}_{fi} = \frac{G_F}{\sqrt{2}} V_{q_{1(2)}q'_{1(2)}} V_{q_3 q'_3} a_1 \mathcal{A}, \tag{12}$$

where $\mathcal{A} = h^\mu H_\mu$, with

$$h^\mu = \sqrt{\frac{2E_{V_2}}{(2\pi)^3}} h'^\mu = \epsilon^{\star\mu}_{V_2}(\vec{q}, \lambda) f_{V_2} m_{V_2} \tag{13}$$

and

$$H_\mu = \frac{1}{\sqrt{N_M(0) N_{V_1}(\vec{k})}} \int \frac{d^3\vec{p}_{q_j} \mathcal{G}_M(\vec{p}_{q_j}, -\vec{p}_{q_j}) \mathcal{G}_{V_1}(\vec{p}_{q_j} + \vec{k}, -\vec{p}_{q_j})}{\sqrt{E_{q_j}(\vec{p}_{q_j}) E_{q'_j}(\vec{p}_{q_j} + \vec{k})}} \times \sqrt{[E_{q_1}(\vec{p}_{q_j}) + E_{q_2}(-\vec{p}_{q_j})][E_{q'_{1(2)}}(\vec{p}_{q_j} + \vec{k}) + E_{q_{2(1)}}(-\vec{p}_{q_j})]} \langle S_{V_1}|J_\mu(0)|S_M\rangle. \tag{14}$$

Using the usual spin algebra, the space and time components of the spin matrix elements $\langle S_{V_1}|J_\mu(0)|S_M\rangle$ in Eq. (14) corresponding to vector and axial-vector currents are obtained as

$$\langle S_{V_1}(\vec{k}, \hat{\epsilon}^*)|V_0|S_M(0)\rangle = 0, \tag{15}$$

$$\langle S_{V_1}(\vec{k}, \hat{\epsilon}^*)|V_i|S_M(0)\rangle = \frac{i\epsilon_{q_j}(\vec{p}_{q_j})}{\sqrt{\epsilon_{q_j}(\vec{p}_{q_j})\epsilon_{q'_j}(\vec{p}_{q_j} + \vec{k})}} (\hat{\epsilon}^* \times \vec{k})_i, \tag{16}$$

$$\langle S_{V_1}(\vec{k}, \hat{\epsilon}^*)|A_i|S_M(0)\rangle = \frac{[\epsilon_{q_j}(\vec{p}_{q_j})\epsilon_{q'_j}(\vec{p}_{q_j} + \vec{k}) - \vec{p}^2_{q_j}/3]}{\sqrt{\epsilon_{q_j}(\vec{p}_{q_j})\epsilon_{q'_j}(\vec{p}_{q_j} + \vec{k})}} \epsilon^*_i, \tag{17}$$

$$\langle S_{V_1}(\vec{k}, \hat{\epsilon}^*)|A_0|S_M(0)\rangle = -\frac{\epsilon_{q_j}(\vec{p}_{q_j})}{\sqrt{\epsilon_{q_j}(\vec{p}_{q_j})\epsilon_{q'_j}(\vec{p}_{q_j} + \vec{k})}} (\hat{\epsilon}^*.\vec{k}). \tag{18}$$

Here for the sake of brevity we use the notation $\epsilon_{q_j}(\vec{p}_{q_j}) = [E_{q_j}(\vec{p}_{q_j}) + m_{q_j}]$ and $\epsilon_{q'_j}(\vec{p}_{q_j} + \vec{k}) = [E_{q'_j}(\vec{p}_{q_j} + \vec{k}) + m_{q'_j}]$, where $E_{q_j}(\vec{p}_{q_j}) = \sqrt{\vec{p}^2_{q_j} + m^2_{q_j}}$ and $E_{q'_j}(\vec{p}_{q_j} + \vec{k}) = \sqrt{(\vec{p}_{q_j} + \vec{k})^2 + m^2_{q'_j}}$ are, respectively, the energy of the non-spectator quark and antiquark. The space component of the hadronic matrix element H_μ obtained from Eq. (14) via Eqs. (16) and (17) are compared with the corresponding expressions from Eqs. (3) and (4) to find the weak form factors $g(q^2)$ and $f(q^2)$,

$$g(q^2) = -\frac{1}{2M} \int d\vec{p}_{q_j} \mathcal{Q}(\vec{p}_{q_j}) \epsilon_{q_j}(\vec{p}_{q_j}), \tag{19}$$

$$f(q^2) = -\int d\vec{p}_{q_j} \mathcal{R}(\vec{p}_{q_j}), \tag{20}$$

where

$$\mathcal{Q}(\vec{p}_{q_j}) = \frac{\mathcal{G}_M(\vec{p}_{q_j}, -\vec{p}_{q_j}) \mathcal{G}_{V_1}(\vec{p}_{q_j} + \vec{k}, -\vec{p}_{q_j})}{\sqrt{N_M(0) N_{V_1}(\vec{k})}} \frac{\sqrt{[E_{q_1}(\vec{p}_{q_j}) + E_{q_2}(-\vec{p}_{q_j})][E_{q'_{1(2)}}(\vec{p}_{q_j} + \vec{k}) + E_{q_{2(1)}}(-\vec{p}_{q_j})]}}{\sqrt{E_{q_j}(\vec{p}_{q_j}) E_{q'_j}(\vec{p}_{q_j} + \vec{k}) \epsilon_{q_j}(\vec{p}_{q_j}) \epsilon_{q'_j}(\vec{p}_{q_j} + \vec{k})}}, \tag{21}$$

$$\mathcal{R}(\vec{p}_{q_j}) = \mathcal{Q}(\vec{p}_{q_j})[\epsilon_{q_j}(\vec{p}_{q_j})\epsilon_{q'_j}(\vec{p}_{q_j} + \vec{k}) - \vec{p}^2_{q_j}/3]. \tag{22}$$

In the present model we also find $a_+(q^2) = a_-(q^2)$. Then the time component of the hadronic amplitude obtained from Eq. (14) via Eq. (18), when compared with the corresponding expression from Eq. (3), gives

$$a_+(q^2) = -\frac{1}{2M^2}\left[E_{V_1} \int d\vec{p}_{q_j} \mathcal{Q}(\vec{p}_{q_j}) \epsilon_{q_j}(\vec{p}_{q_j}) - \int d\vec{p}_{q_j} \mathcal{R}(\vec{p}_{q_j})\right]. \tag{23}$$

It is straightforward to get model expressions for the polarized amplitude squared $|\mathcal{A}_j|^2$ using Eqs. (19)–(22). Summing over possible polarization states and integrating over the final-state particle momenta, the decay width $\Gamma(M \to V_1 V_2)$

is finally obtained in the parent-meson rest frame from the generic expression

$$\Gamma(M \to V_1 V_2) = \frac{1}{(2\pi)^2} \int \frac{d\vec{k} d\vec{q}}{2M 2E_{V_1} 2E_{V_2}} \delta^{(4)}(p - k - q) \times \bar{\sum} |\mathcal{M}_{fi}|^2. \quad (24)$$

Note that we have thus far calculated the color-favored diagram shown in Fig. 1(a) which corresponds to class I nonleptonic decays. Similarly, class II and III $B_c \to VV$ decays can be calculated from the corresponding Feynman diagrams shown in Figs. 1(b) and 1(c), respectively. The model expressions for the weak form factors $g(q^2)$, $f(q^2)$, and $a_+(q^2)$, and hence for the polarized amplitudes in such decays can also be obtained by suitably replacing relevant flavor degrees of freedom, quark masses, meson masses, meson decay constants, the QCD factors a_i, etc.

IV. NUMERICAL RESULTS AND DISCUSSION

For numerical calculations, we take the potential parameters (a, V_0), quark masses "m_q," and corresponding binding energies "E_q" to be those used to describe a wide range of hadronic phenomena in the light- and heavy-flavor sectors [45–48], namely,

$$\begin{aligned}(a, V_0) &\equiv (0.017166\ \text{GeV}^3, -0.1375\ \text{GeV}),\\ (m_u = m_d, m_s, m_c, m_b) &\equiv (0.07875, 0.31575, 1.49276, 4.77659)\ \text{GeV},\\ (E_u = E_d, E_s, E_c, E_b) &\equiv (0.47125, 0.59100, 1.57951, 4.76633)\ \text{GeV}. \end{aligned} \quad (25)$$

The B_c-meson mass and lifetime, as well as the CKM parameters used here, are taken from Ref. [54],

$$\begin{aligned}(M, \tau_{B_c}) &\equiv (6.277\ \text{GeV}, 0.45\ \text{ps}),\\ (|V_{cb}|, |V_{ub}|) &\equiv (0.0412, 0.00393),\\ (|V_{cd}|, |V_{cs}|) &\equiv (0.23, 1.04),\\ (|V_{ud}|, |V_{us}|) &\equiv (0.97418, 0.2255). \end{aligned} \quad (26)$$

The physical masses of the daughter mesons relevant to the decay processes discussed here are set to their observed values [54]. In order to minimize any possible uncertainty in the model calculation due to the values of the relevant meson decay constants, we take their corresponding experimental results or average values from the lattice QCD and QCD sum rules [54–59],

$$(f_\rho, f_{K^\star}, f_{D^\star}, f_{D_s^\star}, f_{J/\psi}) \equiv (0.22, 0.217, 0.245, 0.272, 0.40). \quad (27)$$

For evaluating color-suppressed nonleptonic B_c-meson decays involving ρ^0 in the final state, we take the corresponding decay constant $f_{\rho^0} = f_{\rho^-}/\sqrt{2}$.

At the outset we would like to point out that our intention here is not to achieve a particular quantitative precision with the model prediction, but rather to provide an order-of-magnitude estimation in order to test the applicability of the RIQM in this sector. This is because uncertainty in the theoretical prediction in this sector may come from different factors, such as the model parameters, CKM factors, meson decay constants, QCD factors, etc. In the present analysis we have tried to reduce possible uncertainties in the following manner.

The potential parameters and other model quantities—like quark masses and corresponding quark binding energies—are fixed once at the static-level application of this model [46]; these parameters have been used previously to yield reasonable predictions in a wide range of hadron phenomena in the light- and heavy-flavor sectors [45–48]. As such we do not have any free parameter that could have been fine-tuned from time to time to predict different hadronic properties, as stated above. In a sense, with this set of parameters (fixed previously from hadron spectroscopy) we intend to perform a parameter-free calculation to predict nonleptonic B_c-meson decays in the framework of the RIQM. To minimize uncertainties due to CKM factors and the meson-decay constants, we take the central values of the respective observed data and results from lattice QCD and QCD sum rules [54–59].

With regards to the QCD factors "a_i," different values for "a_1" and significantly different values for "a_2" have been used in the literature. For example, in Ref. [14] the authors used the QCD factors $(a_1^b, a_2^b) = (1.12, -0.26)$ and $(a_1^c, a_2^c) = (1.26, -0.51)$ (which were fixed in Ref. [60]), whereas most earlier calculations used a different set of QCD factors, $(a_1^b, a_2^b) = (1.14, -0.2)$ and $(a_1^c, a_2^c) = (1.2, -0.317)$ (which were fixed by Buras *et al.* in the mid 1980s). We call these two sets of QCD factors Set 1 and Set 2, respectively. In order to gauge the uncertainty in the model predictions, we use both sets in our calculation, as was done in Ref. [45].

Using the input parameters (25)–(27), one can evaluate the weak form factors f, g, and a_+ and study their q^2 dependence from Eqs. (19)–(23). It may be mentioned here that in a self-consistent dynamical approach we extract weak form factors from the overlap integrals of meson wave functions obtained in our model, where a q^2 dependence is automatically ensured (see Refs. [21,22]) in the allowed kinematical range. This is in contrast to most of the approaches of previous models where the weak form factors were determined only at one kinematical point—either $q^2 = 0$ or $q^2 = q^2_{\text{max}}$—and then extrapolated to the allowed kinematical range using some phenomenological ansatz (mainly a dipole or Gaussian).

The q^2 dependence of $g(q^2)$, $f(q^2)$, and $a_+(q^2)$ can also be analyzed from the corresponding expressions for the weak form factors in a dimensionless form,

$$V(q^2) = (M + m_{V_1})g(q^2),$$
$$A_1(q^2) = (M + m_{V_1})^{-1} f(q^2), \quad (28)$$
$$A_2(q^2) = -(M + m_{V_1})a_+(q^2).$$

Our predictions for the q^2 dependence of $V(q^2)$, $\tilde{A}_1(q^2)$, and $A_2(q^2)$ in the allowed kinematical ranges for CKM-enhanced and CKM-suppressed B_c-meson decays are shown in Figs. 2–6, where

$$\tilde{A}_1(q^2) = \left[1 - \frac{q^2}{(M + m_{V_1})^2}\right]^{-1} A_1(q^2). \quad (29)$$

One may naively expect the form factors to satisfy the heavy-quark symmetry relation

$$V(q^2) \simeq A_2(q^2) \simeq \tilde{A}_1(q^2) \quad (30)$$

as an outcome of the HQET. However, our model predictions here do not agree with the heavy-quark symmetry relation (30). This is in agreement with the well-known fact that the heavy-flavor symmetry cannot be strictly used in the B_c-meson sector involving two heavy constituent quarks.

The q^2 dependence of the relevant form factors depends on the kinematics involved in the decay process. In $\bar{c} \to \bar{s}, \bar{d}$ induced decays, we find a nearly flat behavior of $B_c^- \to B^\star$

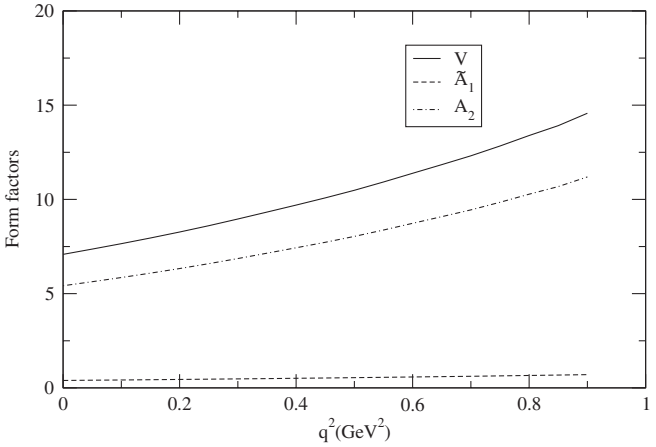

FIG. 2. Form factors of $B_c \to B^\star$.

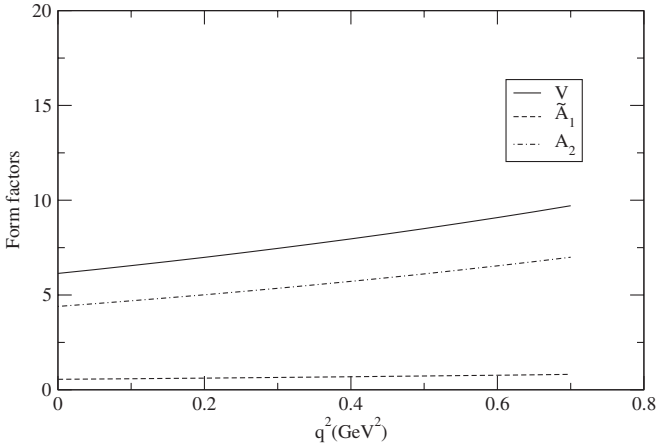

FIG. 3. Form factors of $B_c \to B_s^\star$.

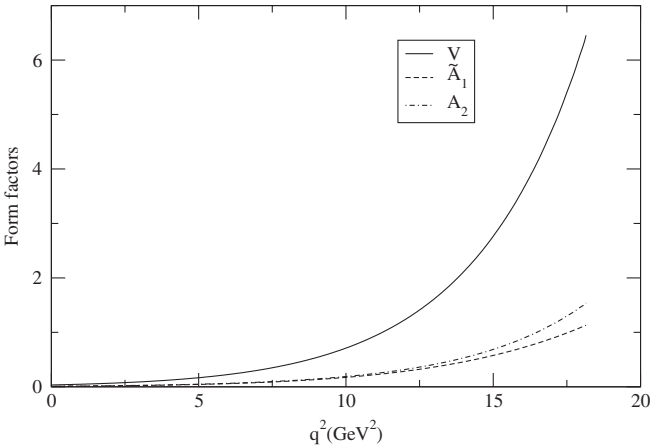

FIG. 4. Form factors of $B_c \to D^*$.

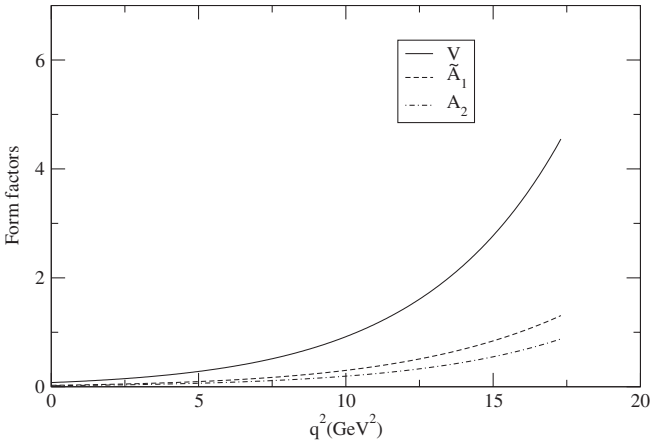

FIG. 5. Form factors of $B_c \to D_s^*$.

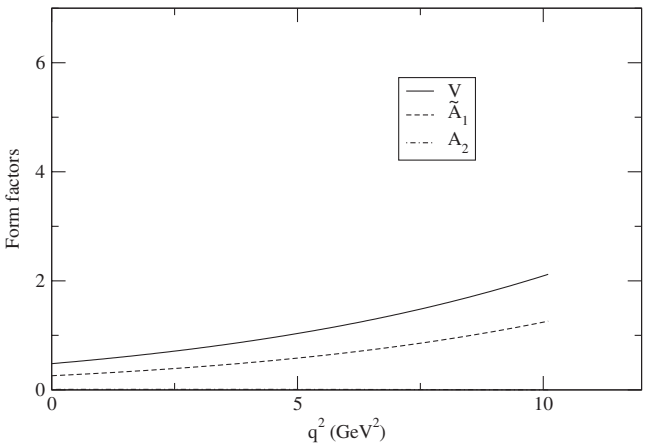

FIG. 6. Form factors of $B_c \to J/\psi$.

and $B_c^- \to B_s^\star$ form factors over the allowed kinematical range (Figs. 2 and 3), since the four-momentum transfers involved in such decays are not too large.

However, in $b \to c$, u induced decays ($B_c^- \to D^\star$, $D_s^\star$, J/ψ), the form factors are found to have a sizeable q^2 dependence, as is evident from the rising slope of the curves in Figs. 4–6 due to the significant momentum transfer involved. As expected, the effect is most pronounced in $B_c \to D^\star$ decays characterized by a maximum recoil momentum of the charmed final state.

Our predictions for the form factors at the maximum recoil ($q^2 = 0$) and zero recoil ($q^2 = q^2_{\rm max}$) points are given in Table I. Our results at $q^2 = 0$ are found to be comparable to those of Ref. [25] for $b \to c$, u induced decay modes, whereas for $\bar{c} \to \bar{s}$, $\bar{d}$ induced modes our predicted values are large compared to their results.

Our predictions for the decay widths $\Gamma(B_c \to VV)$ are listed in Tables II and III for general values of the Wilson coefficients "a_1" and "a_2" to facilitate a comparison with the predictions of other dynamical models. In Tables IV and V, we show our predicted branching ratios for nonleptonic B_c-meson decays to two ground-state vector mesons in comparison with other model predictions. The predicted branching ratios are obtained in a wide range, from tiny values of $\mathcal{O}(10^{-6})$ for $B_c \to D^\star D_{(s)}^\star$ decay modes to a large value of 24.32% for $B_c \to \bar{B}_s^\star \rho^-$.

For $\bar{c} \to \bar{s}$, $\bar{d}$ induced transitions our predicted branching ratios broadly agree with those of Refs. [26,28,30,38]. One may naively expect the bottom-conserving modes to be kinematically suppressed due to the small phase space available. However, the kinematic suppression in these decay modes is overcome due to the large CKM mixing angles involved, ultimately yielding large branching ratios, as shown in Table IV. The most promising decay modes in this category are $B_c^- \to \bar{B}_s^\star \rho^-$ and $B_c^- \to \bar{B}^\star \rho^-$, whose predicted branching ratios are about 24.32% and 1.73%, respectively, which should be experimentally accessible.

Our results for $b \to c$, u induced decay modes such as $B_c \to J/\psi V$ have an order-of-magnitude agreement with those of other dynamical model calculations [21,22,25,26,28,30,33]. The dominant modes in this category are $B_c^- \to J/\psi D_s^{\star -}$ and $B_c \to J/\psi \rho^-$, whose predicted branching ratios are 0.44% and 0.18%, respectively, which should be experimentally accessible at high-luminosity hadron colliders. $B_c \to J/\Psi D_{(s)}^*$ is of particular interest from an experimental point of view. The existing experimental data favor a constructive interference of the color-favored and color-suppressed diagrams in the bottom flavor sector. Since the transition amplitude in $B_c \to J/\Psi D_{(s)}^*$ has contributions from both the diagrams, the predicted branching ratios of these modes would provide an interesting test of interference between the color-favored and color-suppressed B_c decays. Our prediction for the branching ratios of decay modes with two charmed final states such as $B_c \to D^* D_{(s)}^*$ are small compared to those from other models at the same order of magnitude, $\sim\mathcal{O}(10^{-6})$, which is too small to be experimentally accessible.

The relative size of the branching ratios for nonleptonic decays is broadly estimated from a power counting of QCD factors and CKM factors in the Wolfenstein parametrization [62]. Accordingly, the class I decay modes determined by the QCD factor a_1 are found to have comparatively large branching ratios, the most promising of which are the CKM-favored $B_c^- \to \bar{B}_s^* \rho^-$ and $B_c^- \to \bar{B}^* \rho^-$, as shown in

TABLE I. Predicted values of the form factors of weak B_c decays.

Transition	Value at	$V(q^2)$	$A_1(q^2)$	$A_2(q^2)$
$B_c \to J/\psi$	$q^2 = 0$	0.481	0.260	0.010
	$q^2 = q^2_{\rm max}$	2.118	1.26	0.0007
$B_c \to D_s^*$	$q^2 = 0$	0.077	0.026	0.019
	$q^2 = q^2_{\rm max}$	4.54	1.304	0.887
$B_c \to D^*$	$q^2 = 0$	0.034	0.009	0.011
	$q^2 = q^2_{\rm max}$	6.532	1.141	1.560
$B_c \to B_s^*$	$q^2 = 0$	6.131	0.552	4.395
	$q^2 = q^2_{\rm max}$	9.696	0.798	6.984
$B_c \to B^*$	$q^2 = 0$	7.07	0.393	5.409
	$q^2 = q^2_{\rm max}$	14.549	0.685	11.174

TABLE II. Exclusive nonleptonic $B_c \to VV$ decay widths in units of 10^{-15} GeV for general values of the effective Wilson coefficients "a_1" and "a_2."

Quark-level transition	Transition mode	Decay width
$b \to c$, u	$B_c^- \to J/\psi \rho^-$	$2.105a_1^2$
	$B_c^- \to J/\psi K^{*-}$	$0.116a_1^2$
	$B_c^- \to J/\psi D_s^{*-}$	$(2.993a_1 + 3.305a_2)^2$
	$B_c^- \to J/\psi D^{*-}$	$(0.572a_1 + 0.521a_2)^2$
$\bar{c} \to \bar{s}$, $\bar{d}$	$B_c^- \to \bar{B}_s^\star \rho^-$	$224.133a_1^2$
	$B_c^- \to \bar{B}_s^\star K^{*-}$	$7.934a_1^2$
	$B_c^- \to \bar{B}^\star \rho^-$	$15.917a_1^2$
	$B_c^- \to \bar{B}^\star K^{*-}$	$0.507a_1^2$
	$B_c^- \to B^{\star -} \rho^0$	$7.957a_2^2$
	$B_c^- \to B^{\star -} K^{*0}$	$186.06a_2^2$

TABLE III. Exclusive nonleptonic B_c decays into $D^\star D^\star$ mesons in units of 10^{-15} GeV for general values of the effective Wilson coefficients "a_1" and "a_2."

Quark-level transition	Transition mode	Decay width
$b \to c$, u	$B_c^- \to D^{\star -} D^{\star 0}$	$0.170a_2^2$
	$B_c^- \to D_s^{\star -} D^{\star 0}$	$0.031a_2^2$
	$B_c^- \to D^{\star -} \bar{D}^{\star 0}$	$(0.009a_1 + 0.009a_2)^2$
	$B_c^- \to D_s^{\star -} \bar{D}^{\star 0}$	$(0.051a_1 + 0.077a_2)^2$

TABLE IV. Predicted branching ratios (in %) of $B_c \to VV$ decays with the choice of Wilson coefficients Set 1 (Set 2) in comparison with other model predictions.

Decay mode	This work	[33]	[26,38]	[21,22]	[30]	[28]	[40]	[18]
$B_c^- \to J/\psi\rho^-$	0.18 (0.187)	0.21	0.40	0.16	0.31	0.37	0.53	0.49
$B_c^- \to J/\psi K^{\star-}$	0.009 (0.010)	0.016	0.022	0.010	0.018	0.020	0.029	0.028
$B_c^- \to J/\psi D_s^{\star-}$	0.44 (0.53)	0.62	0.67	⋯	0.55	0.59	⋯	0.97
$B_c^- \to J/\psi D^{\star-}$	0.018 (0.021)	0.01	0.028	⋯	0.028	0.019	⋯	0.045
$B_c^- \to \bar{B}_s^{\star}\rho^-$	24.32 (22.06)	12.10	20.2	10.8	16.8	14	14.8	11.0
$B_c^- \to \bar{B}_s^{\star}K^{\star-}$	0.861 (0.781)	⋯	⋯	⋯	1.14	⋯	⋯	0.50
$B_c^- \to \bar{B}^{\star}\rho^-$	1.73 (1.567)	0.67	2.57	0.67	0.89	0.85	1.17	0.30
$B_c^- \to \bar{B}^{\star}K^{\star-}$	0.055 (0.05)	⋯	0.058	0.032	0.065	0.044	0.037	0.013
$B_c^- \to B^{\star-}\rho^0$	0.141 (0.055)	0.031	0.09	0.023	0.031	⋯	0.041	0.011
$B_c^- \to B^{\star-}K^{\star0}$	3.31 (1.278)	0.57	1.67	0.82	1.70	⋯	0.97	0.32

TABLE V. Predicted branching ratios (in 10^{-6}) of $B_c \to D^{\star}D^{\star}$ decays in comparison with other model predictions.

Transition	This work	[18]	[61]	[40]	[35]	[28]	[30]
$B_c^- \to D^{\star-}D^{\star0}$	7.823 (4.629)	21	330	30	55	66	23
$B_c^- \to D_s^{\star-}D^{\star0}$	1.43 (0.846)	1.60	26	1.54	3.50	4.10	1.63
$B_c^- \to D^{\star-}\bar{D}^{\star0}$	0.044 (0.052)	0.20	1.59	⋯	⋯	⋯	⋯
$B_c^- \to D_s^{\star-}\bar{D}^{\star0}$	0.964 (1.276)	4.50	40.40	⋯	⋯	⋯	⋯

Table IV. On the other hand, the branching ratios of class II decay modes determined by a_2 are found to be relatively small, as expected. However, the $B_c^- \to B^{*-}K^{*0}$ decay in this category with CKM factors $V_{cs}V_{ud} \sim 1$ is predicted to have a branching ratio of 3.31%(1.278%), as shown in Table IV, which should be measured experimentally.

In class III decays characterized by the Pauli interference, the branching ratios are determined by the relative values of a_1 with respect to a_2. Considering the negative value of a_2, the decay rates are found to be suppressed, as expected, in comparison with those found when the interference is switched off. However, on a quantitative level the ratio $\frac{a_2}{a_1}$ is a function of the running coupling constant α_s evaluated at the factorization scale, which has been shown [52] to be positive for B decays and negative for D decays, corresponding to small and large couplings, respectively. The experimental data also favor the constructive interference of color-favored and color-suppressed B-decay modes. Taking into account the positive value of $a_2^b = 0.26$ in Set 1 (for example), the predicted branching ratios for the class III B_c decays $B_c \to J/\Psi D_s^{*-}$, $J/\Psi D^{*-}$, $D^{*-}\bar{D}^{0*}$, and $D_s^{*-}\bar{D}^{0*}$ are enhanced by factors of 2.93, 3.03, 2.08, and 4.19, respectively. In order to further probe the effect of Pauli interference in such decays, we put the decay width in the form $\Gamma = \Gamma_0 + \Delta\Gamma$, where $\Gamma_0 = x_1^2a_1^2 + x_2^2a_2^2$ and $\Delta\Gamma = 2x_1x_2a_1a_2$, and then compute the ratios $\frac{\Delta\Gamma}{\Gamma_0}$ for $B_c \to J/\Psi D_s^{*-}$, $J/\Psi D^{*-}$, $D^{*-}\bar{D}^{0*}$, and $D_s^{*-}\bar{D}^{0*}$, which are found to be 48, 50, 44, and 61%, respectively. This indicates that the interference is most significantly involved in the $B_c^- \to D_s^{*-}\bar{D}^{0*}$ decay mode compared to other modes. This is particularly important since such a decay mode has been proposed in Ref. [61] for the extraction of the CKM angle γ through amplitude relations.

Finally, we predict the longitudinal polarization fraction $R_{\rm L}$ and CP-odd fraction $R_\perp$, which are related to the helicity amplitudes by

TABLE VI. Predicted longitudinal polarization fraction $R_{\rm L}$ and the CP-odd fraction $R_\perp$ for $B_c \to VV$ decays in the RIQM.

Quark-level transition	Transition	Longitudinal polarization fraction ($R_{\rm L}$)	CP-odd fraction ($R_\perp$)
$b \to c, u$	$B_c^- \to J/\psi\rho^-$	0.932	0.019
	$B_c^- \to J/\psi K^{*-}$	0.911	0.024
	$B_c^- \to J/\psi D_s^{*-}$	0.570	0.175
	$B_c^- \to J/\psi D^{*-}$	0.590	0.197
	$B_c^- \to D^{\star0}D^{*-}$	0.798	0.157
	$B_c^- \to D^{\star0}D_s^{*-}$	0.796	0.134
	$B_c^- \to \bar{D}^{\star0}D^{*-}$	0.797	0.157
	$B_c^- \to \bar{D}^{\star0}D_s^{*-}$	0.788	0.149
$\bar{c} \to \bar{s}, \bar{d}$	$B_c^- \to \bar{B}_s^{\star}\rho^-$	0.415	0.077
	$B_c^- \to \bar{B}_s^{\star}K^{*-}$	0.333	0.034
	$B_c^- \to \bar{B}^{\star}\rho^-$	0.468	0.252
	$B_c^- \to \bar{B}^{\star}K^{*-}$	0.371	0.164
	$B_c^- \to B^{\star-}\rho^0$	0.467	0.252
	$B_c^- \to B^{\star-}K^{*0}$	0.368	0.157

$$R_{\rm L} = \frac{|A_{ll}|^2}{|A_{+-}|^2 + |A_{-+}|^2 + |A_{ll}|^2},$$
$$R_{\perp} = \frac{|A_{+-} - A_{-+}|^2}{2(|A_{+-}|^2 + |A_{-+}|^2 + |A_{ll}|^2)}. \quad (31)$$

Our results are shown in Table VI. The $b \to c$, u induced decay modes are found predominantly in the longitudinal polarization state, whereas $\bar{c} \to \bar{s}$, $\bar{d}$ induced modes are obtained in slightly higher transverse polarization states. The CP violation in heavy-meson decays such as $B_c \to D^*D^*$, $D_s^*D^*$ is of particular interest as it provides hints for new physics beyond the standard model. This aspect is quantified when predicting $R_\perp$ in such decays. For color-favored $B_c \to D^*(D^*, D_s^*)$ decays, the effect arising due to the short-distance nonspectator contribution is shown to be marginal [63]. However, the long-distance (LD) nonfactorizable contributions from rescattering effects, final-state interactions, etc., may not be negligible. If a significant LD effect exists, one expects a large CP-odd fraction in these decays. The predicted longitudinal and transverse helicity amplitudes and the form factor $g(q^2)$ yield $R_\perp$ values for different $B_c \to VV$ decays, which are shown in Table VI. In particular, the predicted $R_\perp$ values for the transitions with two charmful final states indicate nonvanishing LD contributions, which lead to a significant CP violation in $B_c \to D^*D^*$ and $D^*D_s^*$ decays.

V. SUMMARY AND CONCLUSION

In this paper we investigated the exclusive nonleptonic $B_c \to VV$ decays, within the factorization approximation, in the framework of the RIQM based on a confining potential in an equally mixed scalar-vector harmonic form. We calculated the weak-decay form factors from the overlap integrals of meson wave functions derived in this model. The predicted branching ratios for different decay modes are found in a wide range, from $\mathcal{O}(10^{-6})$ for $B_c \to D^*D_{(s)}^*$ decay modes to the large value of 24.32% for $B_c \to B_s^\star \rho^-$. Our results are in general agreement with those of most of the dynamical quark models, except for some specific modes like $B_c \to D^*D_{(s)}^*$, which are found to be suppressed compared to other model predictions. The decay modes $B_c \to B_s^\star \rho^-$ and $B_c \to B^\star \rho^-$ are found to have large branching ratios of 24.32% and 1.73%, respectively, which should be accessible experimentally. The B_c meson can thus be used as the source of B_s mesons, as the copious production of B_c mesons is expected at the LHC and Tevatron in the near future.

The class I decay modes characterized by the QCD factor a_1 are found to have large branching ratios (as expected) compared to those obtained for class II decays, which are determined by a_2. The branching ratios of class III decays characterized by Pauli interference are found to be too small $\sim\mathcal{O}(10^{-6})$ to be experimentally accessible. The analysis on the effect of interference in such decays indicates that the interference is most significantly involved in the $B_c^- \to D_s^{-*}\bar{D}^{*0}$ decay mode. This is particularly important since the $B_c^- \to D_s^{-*}\bar{D}^{*0}$ decay mode has been proposed for extracting the CKM angle γ through amplitude relations.

The $b \to c$, u induced B_c decays are predominantly found in the longitudinal state, whereas those induced by $\bar{c} \to \bar{s}$, $\bar{d}$ are obtained in slightly higher transverse states. Our predicted CP-odd fractions for the color-favored modes $B_c \to D^{-*}\bar{D}^{0*}$, $D_s^{-*}\bar{D}^{0*}$ indicate a significant CP violation in this sector.

In conclusion, the present analysis shows that the factorization approximation works reasonably well in describing the exclusive nonleptonic $B_c \to VV$ decays in the framework of the RIQM.

[1] F. Abe *et al.* (CDF Collaboration), Phys. Rev. D **58**, 112004 (1998); Phys. Rev. Lett. **81**, 2432 (1998).

[2] T. Aaltonen *et al.* (CDF Collaboration), Phys. Rev. Lett. **100**, 182002 (2008); A. Abulencia *et al.* (CDF Collaboration), Phys. Rev. Lett. **97**, 012002 (2006); **96**, 082002 (2006).

[3] V. M. Abazov *et al.* (D0 Collaboration), Phys. Rev. Lett. **101**, 012001 (2008).

[4] N. Brambilla *et al.* (Quarkonium Working Group), Report No. CERN-2005-005;M. P. Altarelli and F. Teubert, Int. J. Mod. Phys. A **23**, 5117 (2008).

[5] M. Wirbel, B. Stech, and M. Bauer, Z. Phys. C **29**, 637 (1985); M. Bauer, B. Stech, and M. Wirbel, Z. Phys. C **34**, 103 (1987); L.-L. Chau, H.-Y. Cheng, W. K. Sze, H. Yao, and B. Tseng, Phys. Rev. D **43**, 2176 (1991); **58**, 019902 (1998).

[6] A. Ali, G. Kramer, and C. D. Lu, Phys. Rev. D **58**, 094009 (1998); C. D. Lu, Nucl. Phys. B, Proc. Suppl. **74**, 227 (1999).

[7] Y.-H. Chen, H.-Y. Cheng, B. Tseng, and K.-C. Yang, Phys. Rev. D **60**, 094014 (1999); H.-Y. Cheng and K.-C. Yang, Phys. Rev. D **62**, 054029 (2000).

[8] M. Beneke, G. Buchalla, M. Neubert, and C. T. Sachrajda, Phys. Rev. Lett. **83**, 1914 (1999); Nucl. Phys. **B591**, 313 (2000); **B606**, 245 (2001).

[9] Y. Y. Keum, H.-N. Li, and A. I. Sanda, Phys. Lett. B **504**, 6 (2001); Phys. Rev. D **63**, 054008 (2001); C. D. Lu, K. Ukai, and M. Z. Yang, Phys. Rev. D **63**, 074009 (2001); C. D. Lu and M. Z. Yang, Eur. Phys. J. C **23**, 275 (2002).

[10] A. J. Buras, J. M. Gerard, and R. Ruckl, Nucl. Phys. **B268**, 16 (1986).

[11] J. D. Bjorken, Nucl. Phys. B, Proc. Suppl. **11**, 325 (1989).

[12] M. Neubert, Phys. Rep. **245**, 259 (1994).
[13] M. J. Dugan and B. Grinstein, Phys. Lett. B **255**, 583 (1991); C. Reader and N. Isgur, Phys. Rev. D **47**, 1007 (1993).
[14] R. Dhir and R. C. Verma, Phys. Rev. D **79**, 034004 (2009); R. Dhir, N. Sharma, and R. C. Verma, J. Phys. G **35**, 085002 (2008).
[15] J. Sun, D. Du, and Y. Yang, Eur. Phys. J. C **60**, 107 (2009); J. Sun, Y. Yang, W. Du, and H. Ma, Phys. Rev. D **77**, 114004 (2008); J. Sun, G. Xue, Y. Yang, G. Lu, and D. Du, Phys. Rev. D **77**, 074013 (2008).
[16] X. Liu and X. Q. Li, Phys. Rev. D **77**, 096010 (2008).
[17] A. K. Giri, B. Mawlong, and R. Mohanta, Phys. Rev. D **75**, 097304 (2007); **76**, 099902(E) (2007); A. K. Giri, R. Mohanta, and M. P. Khanna, Phys. Rev. D **65**, 034016 (2002); V. V. Kiselev, J. Phys. G **30**, 1445 (2004).
[18] M. A. Ivanov, J. G. Korner, and P. Santorelli, Phys. Rev. D **73**, 054024 (2006).
[19] J. F. Cheng, D. S. Du, and C. D. Lu, Eur. Phys. J. C **45**, 711 (2006).
[20] S. Fajfer, J. F. Kamenik, and P. Singer, Phys. Rev. D **70**, 074022 (2004).
[21] D. Ebert, R. N. Faustov, and V. O. Galkin, Phys. Rev. D **68**, 094020 (2003).
[22] D. Ebert, R. N. Faustov, and V. O. Galkin, Eur. Phys. J. C **32**, 29 (2003).
[23] V. V. Kiselev, O. N. Pakhomova, and V. A. Saleev, J. Phys. G **28**, 595 (2002); V. V. Kiselev, J. Phys. G **30**, 1445 (2004).
[24] G. L. Castro, H. B. Mayorga, and J. H. Munoz, J. Phys. G **28**, 2241 (2002).
[25] R. C. Verma and A. Sharma, Phys. Rev. D **65**, 114007 (2002); **64**, 114018 (2001).
[26] V. V. Kiselev, arXiv:hep-ph/0211021; V. V. Kiselev, A. E. Kovalsky, and A. K. Likhoded, Phys. At. Nucl. **64**, 1860 (2001); Nucl. Phys. **B585**, 353 (2000).
[27] V. A. Saleev, Phys. At. Nucl. **64**, 2027 (2001); O. N. Pakhomova and V. A. Saleev, Phys. At. Nucl. **63**, 1999 (2000).
[28] P. Colangelo and F. DeFazio, Phys. Rev. D **61**, 034012 (2000).
[29] R. Fleischer and D. Wyler, Phys. Rev. D **62**, 057503 (2000).
[30] A. Abd El-Hady, J. H. Munoz, and J. P. Vary, Phys. Rev. D **62**, 014019 (2000).
[31] L. B. Guo and D.-S. Du, Chin. Phys. Lett. **18**, 498 (2001).
[32] Y.-S. Dai and D.-S. Du, Eur. Phys. J. C **9**, 557 (1999).
[33] A. Y. Anisimov, I. M. Narodetskii, C. Semay, and B. Silvestre-Brac, Phys. Lett. B **452**, 129 (1999); A. Anisimov, P. Yu. Kulikov, I. M. Narodetskii, and K. A. Ter-Martirosyan, Yad. Fiz. **62**, 1868 (1999).
[34] D.-S. Du and Z.-T. Wei, Eur. Phys. J. C **5**, 705 (1998).
[35] J. F. Liu and K. T. Chao, Phys. Rev. D **56**, 4133 (1997).
[36] D. S. Du, G. R. Lu, and Y. D. Yang, Phys. Lett. B **387**, 187 (1996).
[37] A. V. Berezhnoy, V. V. Kiselev, A. K. Likhoded, and A. I. Onishchenko, Phys. At. Nucl. **60**, 1729 (1997); S. S. Gershtein, V. V. Kiselev, A. K. Likhoded, A. V. Tkabladze, and A. I. Onishchenko, arXiv:hep-ph/9803433.
[38] V. V. Kiselev, arXiv:hep-ph/9605451.
[39] S. S. Gershtein, V. V. Kiselev, A. K. Likhoded, and A. V. Tkabladze, Phys. Usp. **38**, 1 (1995).
[40] C. H. Chang and Y. Q. Chen, Phys. Rev. D **49**, 3399 (1994).
[41] Q. P. Xu and A. N. Kamal, Phys. Rev. D **46**, 3836 (1992).
[42] M. Masetti, Phys. Lett. B **286**, 160 (1992).
[43] D. S. Du and Z. Wang, Phys. Rev. D **39**, 1342 (1989).
[44] J. D. Bjorken, draft report, 22 July, 1986 (unpublished).
[45] Sk. Naimuddin, S. Kar, M. Priyadarshini, N. Barik, and P. C. Dash, Phys. Rev. D **86**, 094028 (2012).
[46] N. Barik, B. K. Dash, and M. Das, Phys. Rev. D **32**, 1725 (1985); N. Barik and B. K. Dash, Phys. Rev. D **33**, 1925 (1986); **34**, 2092 (1986); **34**, 2803 (1986); N. Barik, B. K. Dash, and P. C. Dash, Pramana J. Phys. **29**, 543 (1987); N. Barik, S. Kar, and P. C. Dash, Pramana J. Phys. **48**, 985 (1997); N. Barik, Sk. Naimuddin, S. Kar, and P. C. Dash, Phys. Rev. D **59**, 037301 (1998).
[47] N. Barik, P. C. Dash, and A. R. Panda, Phys. Rev. D **46**, 3856 (1992); N. Barik and P. C. Dash, Phys. Rev. D **49**, 299 (1994); Mod. Phys. Lett. A **10**, 103 (1995); N. Barik, S. Kar, and P. C. Dash, Phys. Rev. D **57**, 405 (1998); N. Barik, Sk. Naimuddin, S. Kar, and P. C. Dash, Phys. Rev. D **63**, 014024 (2000); N. Barik, P. C. Dash, and A. R. Panda, Phys. Rev. D **47**, 1001 (1993); N. Barik and P. C. Dash, Phys. Rev. D **47**, 2788 (1993); **53**, 1366 (1996); N. Barik, S. K. Tripathy, S. Kar, and P. C. Dash, Phys. Rev. D **56**, 4238 (1997); N. Barik, Sk. Naimuddin, P. C. Dash, and S. Kar, Phys. Rev. D **80**, 074005 (2009); **77**, 014038 (2008); **78**, 114030 (2008); N. Barik, Sk. Naimuddin, and P. C. Dash, Int. J. Mod. Phys. A **24**, 2335 (2009).
[48] N. Barik, S. Kar, and P. C. Dash, Phys. Rev. D **63**, 114002 (2001); N. Barik, Sk. Naimuddin, P. C. Dash, and S. Kar, Phys. Rev. D **80**, 014004 (2009).
[49] I. P. Gouz, V. V. Kiselev, A. K. Likhoded, V. I. Romanovsky, and O. P. Yushchenko, Phys. At. Nucl. **67**, 1559 (2004).
[50] E. Hornandez, J. Nieves, and J. M. Verde-Velasco, Phys. Rev. D **74**, 074008 (2006).
[51] H. M. Choi and C. R. Ji, Phys. Rev. D **80**, 114003 (2009).
[52] M. Neubert and B. Stech, Adv. Ser. Dir. High Energy Phys. **15**, 294 (1998).
[53] C. E. Thomas, Phys. Rev. D **73**, 054016 (2006).
[54] J. Beringer *et al.* (Particle Data Group), Phys. Rev. D **86**, 010001 (2012).
[55] H. N. Li and S, Mishima, Phys. Rev. D **74**, 094020 (2006).
[56] D. Becirevic, Ph. Boucaud, J. Leroy, V. Lubicz, G. Martinelli, F. Mescia, and F. Rapuano, Phys. Rev. D **60**, 074501 (1999).
[57] C. Aubin *et al.* (Fermilab Lattice, MILC, and HPQCD Collaborations), Phys. Rev. Lett. **95**, 122002 (2005).
[58] D. S. Hwang and G.-H. Kim, Z. Phys. C **76**, 107 (1997).
[59] C. Caso *et al.*, Eur. Phys. J. C **3**, 1 (1998).
[60] T. E. Browder and K. Honscheid, Prog. Part. Nucl. Phys. **35**, 81 (1995); M. Neubert, V. Rieckert, B. Stech, and Q. P. Xu, in *Heavy flavors*, edited by A. J. Buras and H. Lindner (World Scientific, Singapore, 1992) and references therein.
[61] V. V. Kiselev, J. Phys. G **30**, 1445 (2004); R. Fleischer and D. Wyler, Phys. Rev. D **62**, 057503 (2000); M. Masetti, Phys. Lett. B **286**, 160 (1992); M. A. Ivanov, J. G. Korner, and O. N. Pakhomova, Phys. Lett. B **555**, 189 (2003).
[62] L. Wolfenstein, Phys. Rev. Lett. **51**, 1945 (1983).
[63] H. N. Li and S. Mishima, Phys. Rev. D **71**, 054025 (2005).